narra j

Short Communication

Lichen substances from *Teloschistes flavicans* (Sw.) Norman: Isolation, crystal structure, and evaluation of their antibacterial activities

Friardi Ismed[1*], Nurwahidatul Arifa[1], Mentari Q. Nissa[1], Deddi P. Putra[1], Analia IC. Orue[2], Jack K. Clegg[2], Isabelle Rouaud[3] and Françoise L. Dévéhat[3]

[1]The Laboratory of Natural Resource of Sumatra (LBS) and Faculty of Pharmacy, Universitas Andalas, Padang, Indonesia; [2]School of Chemistry and Molecular Biosciences, University of Queensland, St Lucia, Queensland, Australia; [3]Centre national de la recherche scientifique (CNRS) Institut des Sciences Chimiques de Rennes (ISCR), Universite de Rennes, Rennes, France

*Corresponding author: friardi@phar.unand.ac.id

Abstract

Teloschistes flavicans (Sw.) Norman is a lichen known as the golden-haired lichen. This lichen has been recognized and used in herbal medicine mixtures as an antimicrobial and bioindicator of air pollution that plays a role in ecological systems. The aim of this study was to explore the potential of its secondary metabolites as antibacterial and anticancer agents, particularly against bacterial pneumonia. Two main compounds (vicacinin and parietin) were isolated with chromatography and identified by spectrometry and single-crystal X-ray diffraction. The crystallographic data of vicanicin are reported for the first time. Chromatography and recrystallization methods were used to obtain both compounds with orange (parietin) and white (vicanicin) crystals. Furthermore, these compounds were evaluated for cytotoxicity on keratinocytes (HaCaT) cells and antibacterial activity against pneumonia pathogens (*Klebsiella pneumoniae* ATCC 1706, *Streptococcus pneumoniae* ATCC 49619, *Moraxella catarhalis* ATCC 25240, and *Staphylococcus pyogenes* ATCC 19615). The cytotoxic activity of these compounds was moderate at the concentration of 50-100 µM. The antibacterial pneumonia activity was relatively weak compared to chloramphenicol. Between the two compounds, vicanicin showed stronger activity than parietin against all strains. Vicanicin was more active against *Klebsiella pneumoniae* and *Staphylococcus pyogenes* with minimum inhibitory concentrations of 156±0.77 µM and 156±0.91 µM, respectively. In this study, comprehensive molecular structures of parietin and vicanicin have been successfully elucidated, and their antibacterial and cytotoxic activities have been provided.

Keywords: Anthraquinone, crystallography, depsidone, lichen, *Teloschistes*

Introduction

Teloschistes flavicans (Sw.) Norman is a group of fruticose lichens widely distributed worldwide. J.M. Norman first described it in 1852 [1,2], and to date, approximately 246 species have been recorded [3]. The habitat of this lichen includes twigs, tree trunks, or rocks. *T. flavicans* (Sw). Norman is one of the identified species of this genus during the survey and exploration of Sumatran lichens in 2020. It is also known as the golden hair-lichen, with characteristic tufted, erect, spreading thallus and yellow to orange in color. *T. flavicans* is also sensitive to air pollution, especially sulfur dioxide [4]. Furthermore, in traditional medicine, this *Teloschistes* genus is used

Received: September 10, 2024 - Accepted: March 24, 2025 - Published online: April 21, 2025

Ismed et al. Narra J 2025; 5 (2): e1463 - http://doi.org/10.52225/narra.v5i2.1463

as a mixed simplicia in "*jamu*" (traditional Indonesian medicine) with significant efficacy as a fever, cough, and headache medicine [5]. Several pharmacological studies have also reported its effects on antidiabetic [6] and antileukemic [7], but also as antimicrobial [8]. These activities are based on the metabolites contained in the thalli. Until now, about 13 metabolites have been isolated from *T. flavicans* (**Figure 1**) [9,10]. Some anthraquinones (parietin, fallacinal, teloschistin), quinone (emodin), monoaromatic phenols (rhizonic acid), and depsidones (isofulgidin, caloploicin, flavicansone, vicanicin) were reported. The content in this species varied according to the location of the species [11].

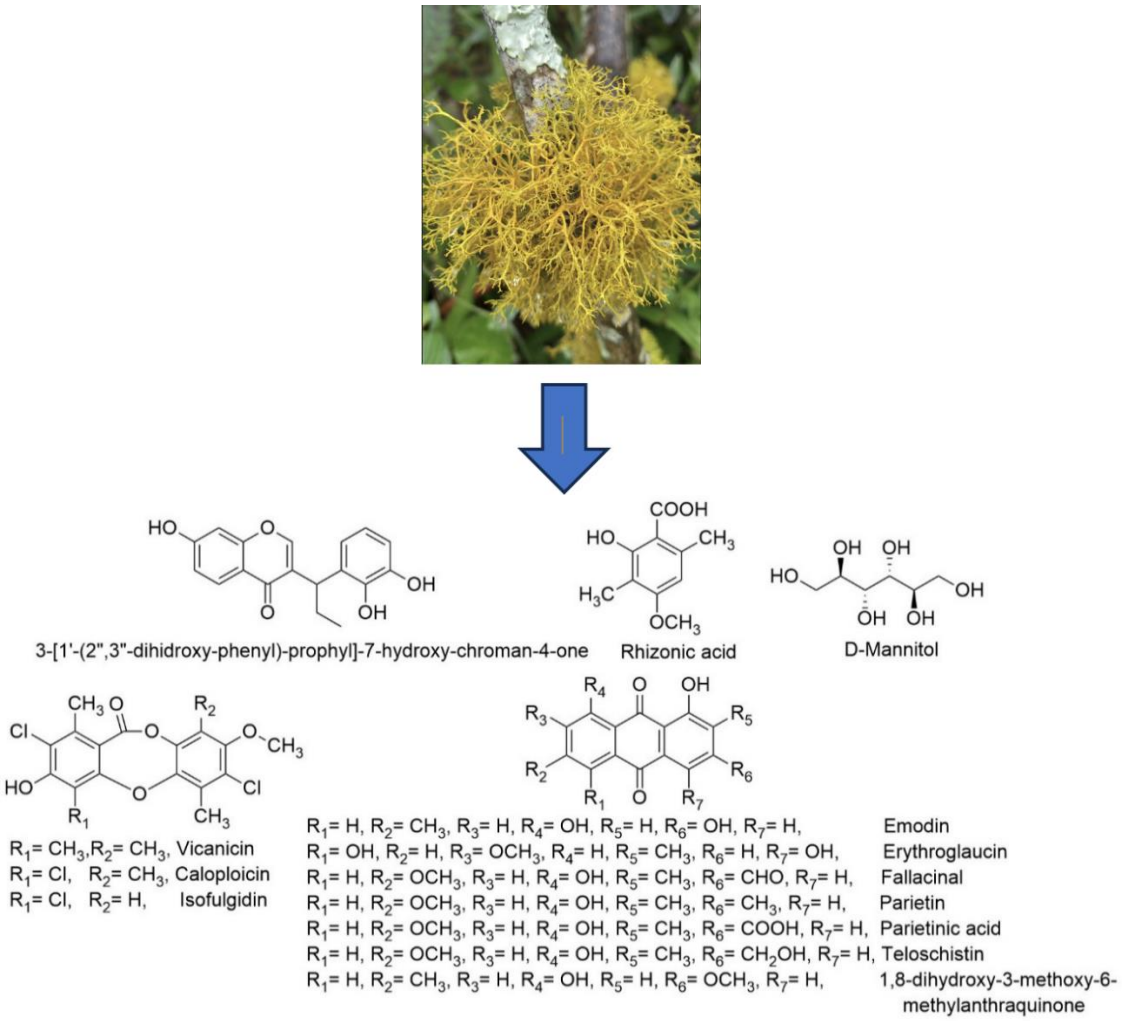

Figure 1. Thallus of *T. flavicans* (top image) and 13 structures of its secondary metabolites.

In a follow-up study on Sumatran lichen exploration [12,13], some thalli of *T. flavicans* were collected in Solok, West Sumatra, Indonesia, and two major compounds were isolated. Their identification was determined using single-crystal X-ray crystallography, and vicanicin and parietin were confirmed to be major metabolites of Indonesian thalli of *T. flavicans*. These compounds were assessed for their effects on keratinocyte cells and their antibacterial activity against pneumonia. Keratinocyte cells, specifically HaCaT cells, serve as a model for evaluating the cytotoxicity of compounds, given the important role of these epithelial cells in body defense and tissue regeneration. This cytotoxicity evaluation was carried out to confirm that compounds from the lichen *T. flavicans* have potential in wound therapy, skin regeneration, or protection against free radical-induced skin damage that leads to skin cancer, especially squamous cell carcinoma or melanoma [14]. Moreover, the pneumonia antibacterial activity assay was conducted using the microdilution method against four pneumonia bacteria (*Klebsiella pneumoniae* ATCC 1706, *Streptococcus pneumoniae* ATCC 49619, *Moraxella catarhalis* ATCC 25240, and *Staphylococcus pyogenes* ATCC 19615). Pneumonia infections caused by these bacteria are a global health problem with high mortality rates, especially in vulnerable groups,

such as children, the elderly, and immunocompromised individuals. The increasing antibiotic resistance to pathogens that cause pneumonia further aggravates the challenges in treatment. Therefore, new and effective therapeutic alternatives are necessary [15]. The aim of this study was to explore the secondary metabolites from the lichen *T. flavicans* and determine their structure by crystallography. Furthermore, it also aims to evaluate its potential as an antiproliferative bioactive compound against keratinocyte cells that may develop into skin cancer, as well as its antibacterial pneumonia activity in inhibiting bacterial growth. There is a lack of crystallographic structure determination of the secondary metabolites from *T. flavicans*, as well as an analysis of their bioactivity as cytotoxic and antibacterial agents for pneumonia.

Methods

Apparatus

The melting point was performed using a Melting Point Apparatus DMP100 (InnotechLab, West Covina, USA) and UV spectra with Shimadzu Pharmaspec 1700 Spectrometer (Shimadzu, Kyoto, Japan) wavelength measurement of 200–400 nm. The Fourier transform-infrared (FT-IR) spectra were obtained on a Perkin Elmer FT-IR Spectrometer (PerkinElmer Inc., Waltham, USA) by KBr pellet technique sampling. High-resolution mass spectrometry measurements were performed on an ACQUITY UPLC and Xevo G2-S QT electron spray ionization with negative mode. ^{1}H- and ^{13}C-Nuclear magnetic resonance (NMR) spectra (500 and 125 MHz) recorded on a JEOL-NMR Spectrometer (JEOL Ltd., Tokyo, Japan) utilize $CDCl_3$ as solvent. The separation was carried out by vacuum liquid chromatography on silica gel (Merck, 35-70µm). Thin layer chromatography (TLC) analyses (Merck, silica gel 60F254) were eluted using some solvent systems: toluene/ethyl acetate/formic acid (139–83–8 v/v/v) (G); n-hexane/ethyl acetate (8–2 v/v/v); toluene/ethyl acetate (8–2 v/v). Visualization was carried out under UV light at 254 and 365 nm, followed by staining with anisaldehyde–H_2SO_4 reagent and subsequent heating.

Lichen specimen

T. flavicans was collected on the stems and twigs of the *Brugmansia arborea* plant in the Danau Kembar tea plantation area, Solok, West Sumatra, Indonesia (0°59'37.9"S, 100°37'59.1"E). The specimen vouchers were stored at the Biota Sumatran Laboratory, Universitas Andalas, West Sumatra, Indonesia, after identification by Dr. Harrie Sipman (Berlin Museum), with the reference numbers TFA 02.

Extraction and isolation

Air-dried thallus powder *T. flavicans* (658 g) was macerated at ambient temperature with three solvents of different polarity (n-hexane, ethyl acetate, and methanol, with a volume of 3 L each, respectively). Furthermore, the n-hexane extract (26.6 g) was subjected to a phytochemical study because the pneumonia antibacterial test (TLC-bioautography) results showed the inhibition of bacterial growth compared to other extracts [16]. After concentration (*in vacuo,* 30°C), an orange crystalline precipitate was formed (2.3 g). It was separated from the filtrate (20.3 g) and then recrystallized in ethyl acetate-n-hexane (ratio 1:1, room temperature), and compound 1 was subjected to single X-ray crystallography. Furthermore, 8 g of the filtrate was chromatographed with vacuum liquid chromatography (160 g silica gel as stationary phase, 5×30 cm^2) with step gradient polarity (n-hexane-ethyl acetate-methanol, v/v, 100 to 0, 0 to 100) as mobile phase. A flow rate of 10 mL/min was used, with fractions collected in 20 mL glass vials and monitored by thin-layer plate chromatography, followed by visualization under UV 254 nm. Eight subfractions were obtained (E1-E8); in the initial subfractions E1 (1.5 g) and E2 (0.9 g), crude needle-like crystals were formed in two different colors, orange and white crystals. The crystals were repeatedly washed with n-hexane and recrystallized with n-hexane-ethyl acetate (1:1). The white needle crystals, called compound 2 (49 mg), and the orange ones (72 mg) were subjected to structural elucidation (UV, IR, MS, NMR) and single-ray crystallography analysis, respectively.

Crystallography

Data were collected using a RigakuOD XtaLAB Synergy with micro-focused MoKα radiation at 100(2) K, wavelength 0.71073 Å, and a Pilatus CdTe 300K detector. The data have been indexed,

reduced, and integrated using CrysAlisPro (Rigaku Oxford Diffraction 2021, Oxford, UK). The structures were solved using SHELXT [17] before refining using SHELXL [18] through the OLEX-2 GUI [19]. Anisotropic refinement was used for non-hydrogen atoms. Carbon-bonded hydrogens were idealized and refined using the Riding model, and oxygen-bonded hydrogens were first located in the Difference-Fourier map. Specific details for each refinement are as follows:

1) Orange crystals (compound 1): $C_{16}H_{12}O_5$ (M=284.26 g/mol), orthorhombic, space group P212121 (no. 19), a=3.7787(5) Å, b=13.554(2) Å, c=23.547(2) Å, V=1206.0(3) Å3, Z=4, T=100.01(10) K, μ(Mo Kα)=0.117 mm^{-1}, Dcalc=1.566 g/cm^3, 8459 reflections measured (4.582°≤2Θ≤56.554°), 2903 unique (Rint=0.0633, Rsigma=0.0785) which were used in all calculations. The final R_1 was 0.0550 (I>2σ(I)), and wR_2 was 0.1459 (all data).
2) White crystals (compound 2): $C_{18}H_{16}Cl_2O_5$ (M =383.21 g/mol), monoclinic, space group P21/c (no. 14), a=23.2178(10) Å, b=3.9450(2) Å, c=17.6187(8) Å, β=93.969(4)°, V=1609.89(14) Å3, Z=4, T=100.00(10) K, μ(Mo Kα)=0.431 mm^{-1}, Dcalc=1.581 g/cm^3, 11510 reflections measured (4.842°≤2Θ≤50.23°), 11510 unique (Rint=0.0637, Rsigma=0.0587) which were used in all calculations. The final R_1 was 0.0890 (I>2σ(I)), and wR_2 was 0.2694 (all data). The structure proved to be twinned by a 180-degree rotation around.

Cytotoxic assay

The evaluation of the cytotoxicity of compounds 1 and 2 was conducted as previously described [20]. HaCaT cells are grown in RPMI 1640 medium (Eurobio L0500-500, Les Ulis, France) supplemented by 5% fetal calf serum (Eurobio CVFSVF00 01D, Les Ulis, France) and 1% antibiotic (Eurobio CABPES01 0U, Les Ulis, France) in 96-plates, in a controlled atmosphere at 5% CO_2 and 37°C. HaCaT cells were seeded at a density of 3,000 cells per well in 96-well plates. Then, the compounds were added. The compounds were diluted in the DMSO biological grade at 50 mM. The stock solutions for compounds (50 mM) were solubilized in DMSO, and then they were diluted in the culture medium (complete RPMI 1640). The final concentrations tested were 100 μM, 50 μM, 25 μM, 10 μM 5 μM and 1 μM. After 48 hours of incubation, 10 μl of MTT was added to each well. Doxorubicin was used as a positive control, and given its high toxicity, the tested concentrations were 0.1–200 μM. Incubation was performed at 37°C for three hours. After the incubation, the plates were centrifuged for five minutes at 1,200 rpm, the supernatant was discarded, and 150 mL of DMSO was added to each well and shaken until the crystals dissolved. The optical density reading was done at 570 nm with the Bio-Rad microplate reader (Bio-Rad Laboratories, USA). Each test was done three times. For each concentration, the mean and the standard deviation were calculated, which makes it possible to construct an effect curve (% of cytotoxicity) according to the concentration. The IC_{50} was determined graphically, a dose that makes it possible to obtain 50% cytotoxicity.

Minimum inhibitory concentration assay

Four respiratory tract infection bacteria were used: *Klebsiella pneumoniae* ATCC 1706, *Streptococcus pneumoniae* ATCC 49619, *Moraxella catarhalis* ATCC 25240, and *Staphylococcus pyogenes* ATCC 19615. The bacterial media was prepared by mixing 1 mL of bacterial suspension (0.5 McFarland) into 30 mL of Mueller-Hinton Agar (MHA) mixed with 5% expired human blood [21], homogenized using a vortex (±1 minute), and then allowed to solidify.

The minimum inhibitory concentration (MIC) values of the isolated compounds were determined using the microdilution method. The MIC determination is based on the lowest concentration that shows no color change after the addition of the iodonitrotetrazolium (INT) (cat. I10406-1G, Merck, Germany) as a bacterial viability indicator. Each isolated compound (compounds 1 and 2) and chloramphenicol as a positive control were dissolved with DMSO and then diluted in Brain Heart Infusion Broth (BHI, Merck, Darmstadt, Germany) to obtain a final concentration that ranged from 1,000–10 μM. Furthermore, each well of a 96-well microplate received 100 μl of the test solution in triplicate. Thereafter, 5 μl of bacterial suspension (1×10^6 CFU/ml) was added to each well. The microplate was incubated at 36°C for 18 hours. After incubation, 20 μl of INT in ethanol 70% (0.5 mg/ml) was added to each well and incubated for 30 minutes. Color change detection was performed using spectrophotometry at a wavelength of 600 nm (Bio-Rad microplate reader, Bio-Rad Laboratories, USA). Complete inhibition of bacterial growth was indicated by the absence of color change.

Results

Structure elucidation with spectroscopy

The isolated compounds, vicanicin and parietin, were identified using spectroscopic techniques, including FT-IR, UV-Vis, LC-MS, and ^{1}H-^{13}C-NMR. Compound 1 appeared as orange needle-like crystals in $CHCl_3$, with a melting point of 205–207°C. Its UV-Vis absorption maxima were observed at 267, 283.5, and 433 nm. The infrared (IR) spectrum showed characteristic peaks at 2,932, 1,611, 1,374, 1,229, 1,140, and 1,032 cm^{-1}. ESIMS (negative mode) revealed an $[M-H]^-$ ion at m/z 283.0605, consistent with the molecular formula $C_{16}H_{12}O_5$. Meanwhile, compound 2 appeared as white needle-like crystals in $CHCl_3$, with a melting point of 249°C. Its UV-Vis absorption maximum was recorded at 268 nm. The IR spectrum (KBr) exhibited peaks at 3,416, 1,731, 1,255, and 842 cm^{-1}. ESIMS (negative mode) showed an $[M-H]^-$ ion at *m/z* 381.0289, corresponding to the molecular formula $C_{18}H_{15}Cl_2O_5$. The NMR data for both compounds are summarized and presented in **Table 1**.

Table 1. Nuclear magnetic resonance (NMR) data of compound 1 and compound 2 isolated from *Teloschistes flavicans*

#	Compound 1		#	Compound 2	
	^{13}C-NMR (125 MHz, $CDCl_3$) δC (ppm)	^{1}H-NMR (500 MHz, $CDCl_3$) δH (ppm)		^{13}C-NMR (125 MHz, $CDCl_3$) δC (ppm)	^{1}H-NMR (500 MHz, $CDCl_3$) δH (ppm)
C1	162.574	12.305 (1H,s,-OH),	C1	114.484	
C2	124.601	6.674 (1H,d,J=2),	C2	159.579	
C3	148.541		C3	115.358	
C4	121.386	7.349(1H,d,J=2.5)	C4	153.532	
C5	136.314		C5	118.756	
C6	182.136		C6	146.592	
C7	133.279		C7	162.862	
C8	108.322	7.610 (1H,d,J=2),	C8	10.771	2.411 (3H,s),
C9	165.262		C9	14.850	2.489 (3H,d,J=5)
C10	106.844	7.066 (1H,s),	C1’	125.283	
C11	166.625	12.106 (1H,s,-OH),	C2’	152.063	
C12	110.328		C3’	122.471	
C13	190.880		C4’	142.081	
C14	113.745		C5’	138.212	
C15	22.251	2.436 (3H,s),	C6’	126.857	
C16	56.172	3.924(3H,s,OCH3)	C7’	10.348	2.291 (3H,s),
			C8’	18.641	2.479 (3H,d,J=5)
			C9’	60.482	3.753 (3H,s)

Structure elucidation with single X-ray crystallography

Compound 1 crystallizes in the orthorhombic space group $P2_12_12_1$ with one molecule in the asymmetric unit (**Figure 2A**). Integrating the spectroscopic and crystallographic data results confirms that compound 1 is parietin. Compound 2 crystallizes in the monoclinic space group $P2_1/c$ with one molecule in the asymmetric unit (**Figure 2B**). The two phenyl rings of the molecule are inclined at 125.46° to each other, resembling a gable-shaped motif. Compound 2 was identified as vicanicin, and its crystallographic data were reported for the first time.

Cytotoxic and anti-pneumonia assays

Parietin and vicanicin were tested on keratinocyte cells to evaluate the cytotoxic activities on normal cells (**Figure 3**) and also on pneumonia strains to evaluate their antibacterial effects (**Table 2**). A dose-dependent cytotoxicity relationship was observed (**Figure 3**), where parietin exhibited higher cytotoxicity at low concentrations on normal cells than vicanicin, even at a concentration of 1 µM. Vicanicin was more toxic at high concentrations (100 µM, 50 µM) than parietin, but this difference in intensity decreased from 25 µM. Nevertheless, this effect was lower compared to the anticancer drug doxorubicin, whose IC_{50} was 0.45±0.12 µM. The antimicrobial activity of both compounds was tested against four bacterial strains (**Table 2**), revealing relatively weak inhibition compared to the positive control, chloramphenicol. Vicanicin showed stronger activity than parietin against all strains, and it was more active against *K. pneumoniae* (MIC=156±0.77 µM) and *S. pyogenes* (MIC=156±0.91 µM).

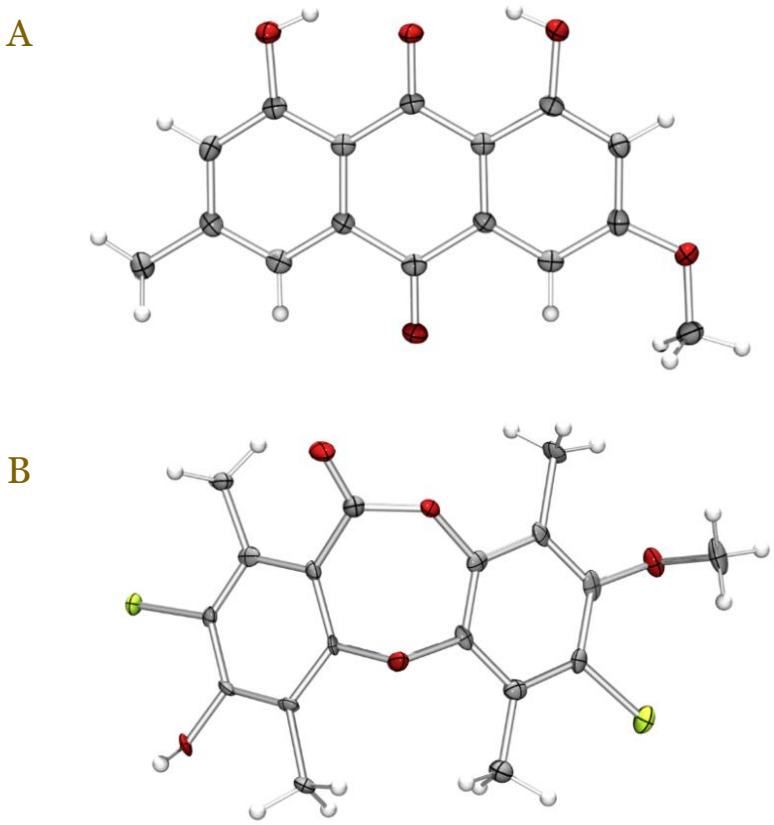

Figure 2. ORTEP representation of the crystal structure of parietin (A) and vicanicin (B), shown with 50% probability of ellipsoids, adopted from a previous study [12].

Table 2. Antipneumonia effect of parietin and vicanicin on four bacterial strains expressed in minimum inhibitory concentration (MIC)

Bacteria	MIC (µM)		
	Parietin	Vicanicin	Chloramphenicol
Klebsiella pneumoniae	354±0.27	156±0.77	15±0.33
Streptococcus pneumoniae	333±0.02	261±0.18	13±0.13
Staphylococcus pyogenes	352±0.35	156±0.91	14±0.55
Moraxella catarrhalis	350±0.71	261±0.57	15±0.21

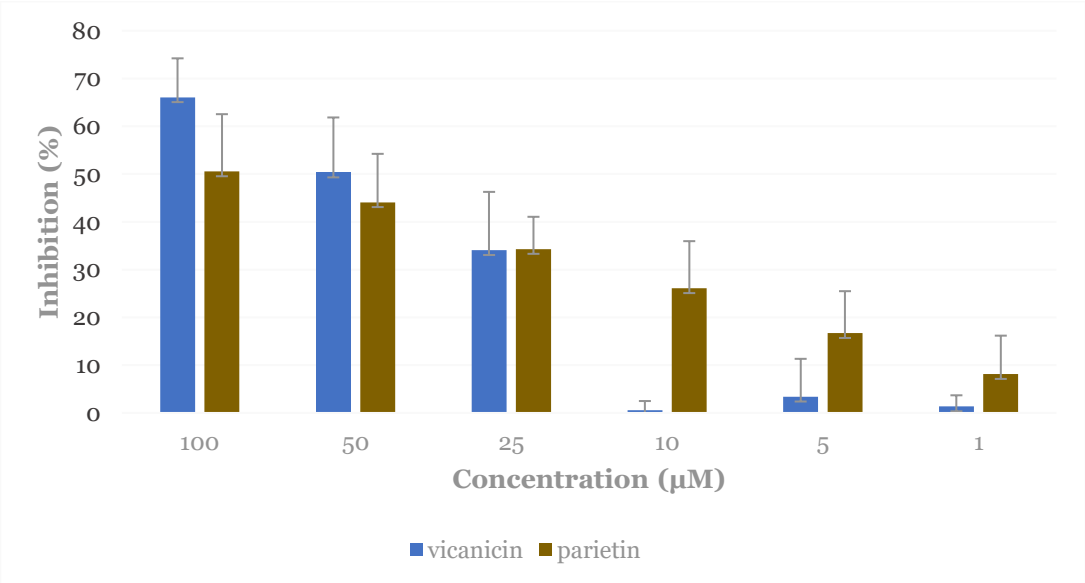

Figure 3. Cytotoxic activities on keratinocyte cells (HaCaT) for vicanicin and parietin.

Discussion

The structural elucidation of parietin, as confirmed by spectroscopic and single-crystal X-ray crystallography data, aligns with previous reports on anthraquinone derivatives [22]. The UV-Vis analysis indicated characteristic absorption peaks at 267–268 nm, which correspond to π-π* electronic transitions typical of anthraquinones. FT-IR spectroscopy further revealed key functional groups, including hydroxyl (-OH), ketone (-C=O), and aromatic C=C bonds, supporting the presence of an anthraquinone core. Mass spectrometry data confirmed the molecular formula $C_{16}H_{12}O_5$, with fragmentation patterns consistent with known anthraquinones, demonstrating stability in ionization conditions. The fragmentation data were compared with the report by Zhan and colleagues [22].

^{1}H- and ^{13}C-NMR spectra provided detailed insights into the molecular framework of parietin. The presence of a methyl (-CH_3) signal at δH of 2.43 ppm and a methoxy (-OCH_3) group at δH of 3.92 ppm suggests modifications that may influence its bioactivity. The downfield chemical shifts at δH of 12.10 and 12.30 ppm indicate hydroxyl (-OH) groups capable of forming hydrogen bonds, which could contribute to the molecular interactions observed in the crystallographic study.

The structure of parietin obtained is consistent with that previously reported for spectroscopic analyses [23] and for crystallographic data at 193 K [24]. The crystal packing shows a 1D-chain of π-stacked molecules with an interplanar distance of 3.42 Å, in addition to intermolecular C-H···O hydrogen bonding. The 1D chains are connected by O-H···O (2.39 Å, ∠OHO 128.4°) hydrogen bonding interactions between the alcohol groups of neighboring molecules to form a zigzag motif. Additionally, these alcohol groups also form intramolecular hydrogen bonds with the adjacent ketone. There are a number of weaker non-classical CH_3-O hydrogen bonds throughout the lattice (**Figure 4**).

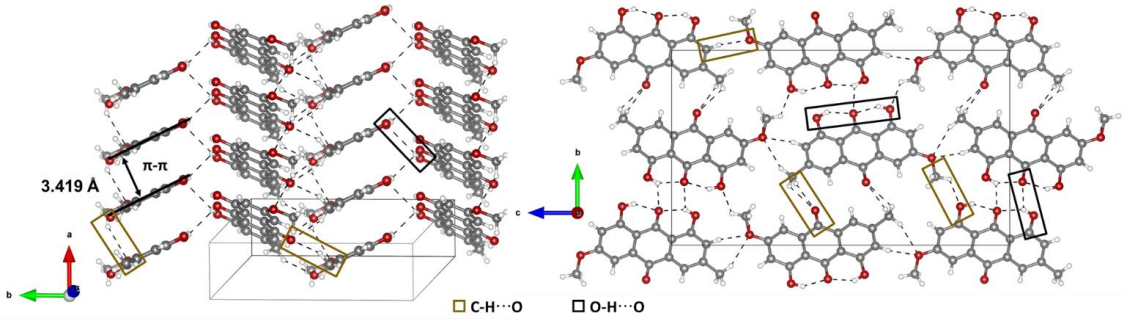

Figure 4. Crystal packing features of compound 1, as suggested by refinement with the least-squares method using SHELXT, before further refinement through the OLEX-2 GUI.

The FT-IR spectral data of vicanicin showed typical absorption for phenolic, carbonyl (C=O), ester, and halogen functional groups at wavenumbers 3,416, 1,731, 1,255, and 842 cm^{-1}, respectively. The molecular formula is $C_{18}H_{15}Cl_2O_5$ on the basis of the ESIMS *m/z* 381.0289 [M-H]- calculated for $C_{18}H_{15}Cl_2O_5$, and the presence of two halogen atoms (Cl) in the structure of compound 2 is indicated by two typical spectral peaks at *m/z* 381.0294 and 383.0268. The presence of chlorine atoms can be confirmed based on typical isotope peak patterns. When chlorine is present in a molecule, the molecular ion peak (*M*+) and its fragment peak will appear in two peaks that have a difference of 2 atomic mass units (Da) in a ratio of 3:1. This is due to the combination of the abundance of ^{35}Cl and ^{37}Cl isotopes [25]. Moreover, the difference in mass between [M] and [M+1] and between [M] and [M+2] is close to 1.997, taking into account the difference between ^{35}Cl-^{37}Cl [26].

The vicanicin compound exhibits a ^{1}H-NMR spectrum with 16 protons. The chemical shifts at 2.291 ppm (3H, s) and 2.411 ppm (3H, s) indicate hydrogen atoms from methyl groups (CH_3), while 2.484 ppm (2×3H, d, J: 5) suggest methyl groups adjacent to each other with a coupling constant of 5. The chemical shift at 3.753 ppm (3H, s) signifies the presence of a methoxy group (-O-CH_3), whereas 6.186 ppm (1H, s) indicates a hydroxyl group (-OH). As for the ^{13}C-NMR, its spectra display 18 carbon signals. The chemical shifts at 114.484 ppm, 115.358 ppm, 118.756 ppm, 122.471 ppm, 125.283 ppm, 126.857 ppm, 138.212 ppm, 142.081 ppm, 146.592 ppm, 152.063

ppm, 153.532 ppm, and 159.579 ppm indicate the presence of carbon atoms forming an aromatic ring. Meanwhile, the chemical shift at 162.862 ppm signifies the presence of a ketone carbon.

Adjacent molecules form one-dimensional chains through π-stacking interactions along the crystallographic b-axis with interplanar distances of 3.40 Å and 3.56 Å. There are a number of intermolecular interactions present between the chains with both O-H···O hydrogen bonds (2.08 Å, ∠OHO 150.9°) and type α halogen bonding [27] Cl···Cl (3.52 Å, (θ1=117.6°, θ2=86.8°, ψ=0.01) (**Figure 5**). CCDC 2428248-2428249 contains the supplementary crystallographic data presented in this paper [28].

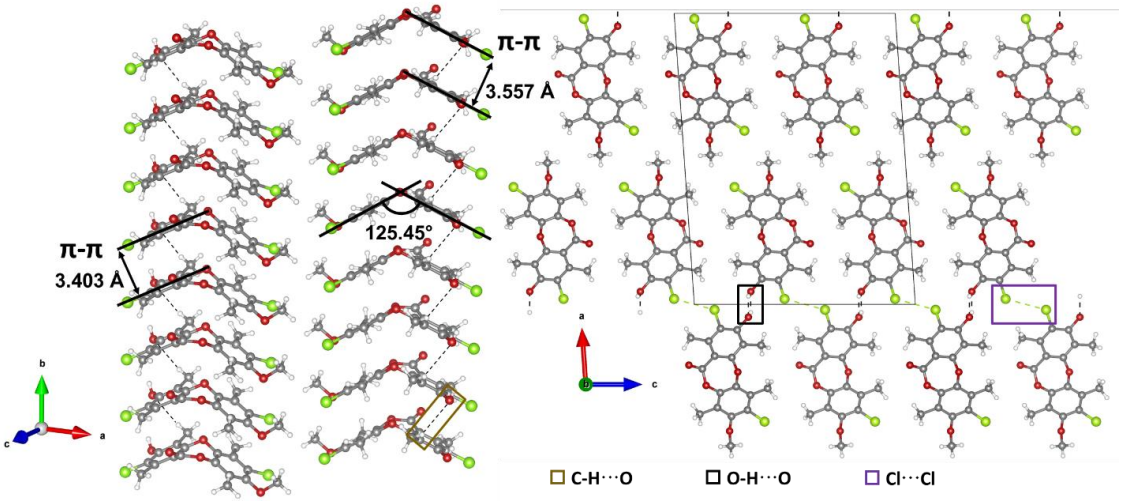

Figure 5. Crystal packing features of compound 2, as suggested by refinement with the least-squares method using SHELXT, before further refinement through the OLEX-2 GUI.

Vicanicin belongs to the depsidone family and was first isolated in 1959 [29]. From the literature, several lichen genera were recorded to contain vicanicin, such as the genus *Teloschistes* [29], *Caloplaca* [30], *Erioderma* [31], and *Psoroma* [32]. Among the metabolites already described in the genus *Teloschistes*, several compounds belong to the anthraquinone family, and all of them appeared orange in color [10,33]. Moreover, several chlorinated compounds are described in *T. flavicans* (caloploicin, isofulgidin, vicanicin), and the single X-ray crystallography allows us to determine unambiguously the structure of both compounds isolated in these thalli. X-ray crystallography is one of the reliable and precise techniques for determining the three-dimensional structure of a molecule, especially on an atomic scale. Some of its advantages are the accurate mapping of atoms and the identification of chemical bonds and electronic properties [34].

Few published articles reported cytotoxic activities for vicanicin and parietin isolated from *T. flavicans* compared with the biological evaluation of extracts [7,35,36]. Among them, an article reported that its methanol extract exhibited a termicidal activity, with vicanicin suspected to play a role [35]. A similar range of cytotoxicity was observed for the n-hexane and ethyl acetate extracts from *T. flavicans* on leukemia cells HL-60. If we postulated that these fractions are enriched in vicanicin and parietin, as they are major compounds, our results are correlated with this assumption. These compounds are toxic at around 50–100 μM for vicanicin and at lower concentrations for parietin [7]. This lower cytotoxic activity was also observed in a previous study, where UVA-blue light irradiation was found to increase the toxicity of parietin [36]. The study further suggests that the effect could be utilized for photo-induced antibacterial effect [36].

This study has described the secondary metabolites of *T. flavicans*, elaborating on their structural characteristics and pharmacological activity. However, several limitations must be acknowledged, including the fact that the pharmacological evaluation remains at the initial in vitro screening stage. Additionally, the study did not assess the potential synergistic effects of these compounds with existing antimicrobial or cytotoxic agents, which could influence their efficacy. Further research is required to investigate the specific mechanisms of action and to develop a more comprehensive understanding of their potential therapeutic applications.

Conclusion

This study successfully isolated vicanicin and parietin in the Indonesian species of *T. flavicans*, and the crystallography data confirmed their structures. The structure determination of vicanicin using the single X-ray crystallography method is reported for the first time. The bioactivity assay showed that both compounds exhibit dose-dependent moderate cytotoxic activities on normal cells, with parietin being more toxic at lower concentrations compared to vicanicin. Meanwhile, their antibacterial inhibition against pneumonia-associated bacteria was relatively weak. Further synergistic evaluations should be investigated after UV irradiation to valorize the potential of these lichen compounds in antibacterial activity.

Ethics approval

Not required

Acknowledgments

This research was funded by the PHC–Nusantara and PRPB scheme of the Ministry of Education, Culture, Research, and Technology-LPDP and the French Ministère de l'Europe et de l'Affaires Etrangères, the French Ministère de l'Éducation. (contract no.011/E5/PG.02.00/PRPB BATCH 2/2024 to FI and project number: 47064PL to FLD)). We are grateful to Dr Harrie J. M. Sipman, Botanischer Garten und Botanisches Museum Berlin-Dahlem, Freie Universität Berlin, for the identification of the lichen. We would also like to thank Azhar Darlan, Puslab for Mabes Polri, for the LC-MS/MS analysis.

Competing interests

All authors declare that no conflicts of interest exist.

Funding

PHC–Nusantara and PRPB scheme of the Ministry of Education, Culture, Research, and Technology-LPDP and the French Ministère de l'Europe et de l'Affaires Etrangères, the French Ministère de l'Éducation (contract no.011/E5/PG.02.00/PRPB BATCH 2/2024 to FI and project number: 47064PL to FLD).

Underlying data

Derived data are available upon request from the corresponding author to support the findings of this study.

Declaration of artificial intelligence use

This study used artificial intelligence (AI) tools and methodologies in the following capacities: Manuscript writing support: AI-based language models, such as ChatGPT and Deepl, were employed for language refinement (improving grammar, sentence structure, and readability of the manuscript). We confirm that all AI-assisted processes were critically reviewed by the authors to ensure the integrity and reliability of the results. The final decisions and interpretations presented in this article were solely made by the authors.

How to cite

Ismed F, Arifa N, Nissa MQ, *et al*. Lichen substances from *Teloschistes flavicans* (Sw.) Norman: Isolation, crystal structure, and evaluation of their antibacterial activities. Narra J 2025; 5 (2): e1463 - http://doi.org/10.52225/narra.v5i2.1463.

References

1. Norman JM. Conatus praemissus redactionis novae generum nonnullorum lichenum in organis fructificationes vel sporis fundatae. Nytt Mag Naturvidenskaberne 1853;7:213-252.
2. Almborn O. Revision of the lichen genus *Teloschistes* in central and southern Africa. Nord J Bot 1989;8:521-538.
3. Index Fungorum. Home page. Available from: http://www.indexfungorum.org. Accessed: 1 January 2025.

4. Gilbert O, Purvis O. *Teloschistes flavicans* in Great Britain: Distribution and ecology. Lichenol 1996;28:493-506.
5. Kusmoro J, Noer IS, Jatnika MF, *et al*. Lichen diversity in geothermal area of Kamojang, Bandung, West Java, Indonesia and its potential for medicines and dyes. Biodiversitas 2018;19:2335-2343.
6. Maulidiyah M, Darmawan A, Hasan A, *et al*. Isolation, structure elucidation, and antidiabetic test of vicanicin compound from lichen *Teloschistes flavicans*. J Appl Pharm Sci 2020;10(11):001-009.
7. Sanjaya A, Avidlyandi A, Adfa M, *et al*. A new depsidone from *Teloschistes flavicans* and the antileukemic activity. J Oleo Sci 2020;69(12):1591-1595.
8. Mishra G, Nayaka S, Upreti D, *et al*. Species and chemical diversity in lichen family Teloschistaceae, and their bioprospecting potential: A review in Indian context. Crypto Biodiv Assess 2018;3(2):8-22.
9. Ferron S, Ismed F, Elyashberg ME, *et al*. CASE-DFT structure elucidation of proton-deficient chlorodepsidones from the Indonesian lichen *Teloschistes flavicans* and structure revision of flavicansone. J Nat Prod 2024;87(9):2148-2159.
10. Canaviri P, Bergquist KE, Vila J. Estudio fitoquímico del liquen *Teloschistes flavicans*. Rev Bol Quím 2006;23:9-12.
11. Søchting U, Frödén P. Chemosyndromes in the lichen genus *Teloschistes* (Teloschistaceae, Lecanorales). Mycol Progress 2002;1:257-266.
12. Ismed F, Farhan A, Bakhtiar A, *et al*. Crystal structure of olivetolic acid: A natural product from *Cetrelia sanguinea* (Schaer.). Acta Crystallogr Sect E Crystallogr Commun 2016;72(Pt 11):1587-1589.
13. Ismed F, Arifa N, Zaini E, *et al*. Ethyl haematommate from *Stereocaulon graminosum* Schaer.: Isolation and crystal structure. Nat Prod Sci 2018;24(2):115-118.
14. Baczewska I, Hawrylak-Nowak B, Zagórska-Dziok M, *et al*. Towards the use of lichens as a source of bioactive substances for topical applications. Molecules 2024;29(18):4352.
15. Li Y, Kumar S, Zhang L. Mechanisms of antibiotic resistance and developments in therapeutic strategies to combat *Klebsiella pneumoniae* infection. Infect Drug Resist 2024;17:1107-1119.
16. Nissa MQ. Isolasi dan karakterisasi metabolit sekunder lichen *Teloschistes flavicans* (sw) Norman serta uji aktivitas antibakteri. Padang: Diploma Thesis Universitas Andalas; 2021.
17. Sheldrick G. SHELXT – integrated space-group and crystal structure determination. Acta Crystallogr Sect A Found Adv 2015;71:3-8.
18. Sheldrick G. A short history of SHELX. Acta Crystallogr Sect A Found Crystallogr 2008;64:112-122.
19. Dolomanov O, Bourhis L, Gildea R, *et al*. OLEX2: A complete structure solution, refinement and analysis program. J Appl Cryst 2009;42:339-341.
20. Ismed F. Phytochimie de lichens du genre Stereocaulon: Étude particulière de *S. Halei* Lamb et *S. montagneanum* Lamb, deux lichens recoltés en Indonésie. Sciences pharmaceutiques. Rennes: PhD Thesis Université Rennes; 2012.
21. Juariah S, Darmadi D, Irawan MP, *et al*. Expired human blood as an alternative substituent of sheep blood for *Streptococcus* sp. growth. J Phys Conf Ser 2019;1175:012012.
22. Zhan C, Xiong A, Shen D, *et al*. Characterization of the principal constituents of Danning Tablets, a Chinese formula consisting of seven herbs, by an UPLC-DAD-MS/MS approach. Molecules 2016;21(5):631.
23. Edwards HGM, Newton EM, Wynn-Williams DD, *et al*. Molecular spectroscopic studies of lichen substances 1: Parietin and emodin. J Mol Struct 2003;648:493-506.
24. Ulický L, Kožíšek J, Ječný J. Structure of an anthracene derivative. Acta Crystallogr Sect C Struct Chem 1991;47:1879-1881.
25. Tang C, Peng L, Tan J, *et al*. Observation of varied characteristics of chlorine isotope effects of organochlorines in dechlorination reactions on different types of electron ionization mass spectrometers. Int J Mass Spectrom 2020;447:116238.
26. Roullier C, Guitton Y, Valery M, *et al*. Automated detection of natural halogenated compounds from LC-MS profiles–application to the isolation of bioactive chlorinated compounds from marine-derived fungi. Anal Chem 2016;88(18):9143-9150.
27. Setter C, Whittaker J, Brock A, *et al*. Straightening out halogen bonds. CrystEngComm 2020;22:1687-1690.
28. Cambridge Crystallographic Data Centre. Search - access structures. Available from: www.ccdc.cam.ac.uk/data_request/cif. Accessed: 1 January 2025.
29. Neelakantan S, Seshadri TR, Subramanian SS. Constitution of vicanicin from the lichen. Tetrahedron Lett 1959;1(9):1-4.
30. Yosioka I, Hino K, Fujio M, *et al*. The structure of caloploicin, a new lichen trichloro-depsidone. Chem Pharm Bull 1973;21(7):1547-1553.

31. Quilhot W, Didyk B, Gambaro V, *et al*. Studies on Chilean lichens, VI. Depsidones from *Erioderma chilense*. J Nat Prod 1983;46(6):942-943.
32. Quilhot W, Piovano M, Arancibia. Studies on Chilean lichens, XII. Chemotaxonomy of the Genus *Psoroma*. J Nat Prod 1989;52(1):191-192.
33. Maulidiyah M, Hasan A, Irna W, *et al*. Antifungal potential against *Aspergillus flavus*: Secondary metabolite compound from unique organism of lichen *Teloschistes flavicans*. Int Res J Pharm 2018;9(8):30-35.
34. Arvalho AL, Trincão J, Romão MJ. X-ray crystallography in drug discovery. In: Roque ACA, editor. Ligand-macromolecular interactions in drug discovery. Methods in molecular biology. Totowa, NJ: Humana Press; 2010.
35. Avidlyandi A, Adfa M, Yudha S. Antitermite activity of methanol extract of lichen *Teloschistes flavicans* (Sw) Norman against *Coptotermes curvignathus*. J Phys Conf Ser 2021;1731:012022.
36. Cogno IS, Gilardi P, Comini L, *et al*. Natural photosensitizers in photodynamic therapy: In vitro activity against monolayers and spheroids of human colorectal adenocarcinoma SW480 cells. Photodiagnosis Photodyn Ther 2020;31:101852.